IOPscience iopscience.iop.org

Home Search Collections Journals About Contact us My IOPscience

Numerical study of the lateral resolution in electrostatic force microscopy for dielectric samples

This article has been downloaded from IOPscience. Please scroll down to see the full text article.

2011 Nanotechnology 22 285705

(http://iopscience.iop.org/0957-4484/22/28/285705)

View the table of contents for this issue, or go to the journal homepage for more

Download details:
IP Address: 128.32.182.17
The article was downloaded on 07/12/2011 at 18:10

Please note that terms and conditions apply.

Nanotechnology 22 (2011) 285705 (6pp) doi:10.1088/0957-4484/22/28/285705

Numerical study of the lateral resolution in electrostatic force microscopy for dielectric samples

C Riedel[1,2,3], A Alegría[1,4], G A Schwartz[4], J Colmenero[1,2,4] and J J Sáenz[2,3]

[1] Departamento de Física de Materiales UPV/EHU, Facultad de Química, Apartado 1072, 20080 San Sebastián, Spain
[2] Donostia International Physics Center, Paseo Manuel de Lardizábal 4, 20018 San Sebastián, Spain
[3] Departamento de Física de la Materia Condensada and Instituto 'Nicolás Cabrera', Universidad Autónoma de Madrid, Campus de Cantoblanco, 28049 Madrid, Spain
[4] Centro de Física de Materiales CSIC-UPV/EHU, Paseo Manuel de Lardizábal 5, 20018 San Sebastián, Spain

E-mail: riedel@ies.univ-montp2.fr

Received 24 February 2011, in final form 7 May 2011
Published 7 June 2011
Online at stacks.iop.org/Nano/22/285705

Abstract
We present a study of the lateral resolution in electrostatic force microscopy for dielectric samples in both force and gradient modes. Whereas previous studies have reported expressions for metallic surfaces having potential heterogeneities (Kelvin probe force microscopy), in this work we take into account the presence of a dielectric medium. We introduce a definition of the lateral resolution based on the force due to a test particle being either a point charge or a polarizable particle on the dielectric surface. The behaviour has been studied over a wide range of typical experimental parameters: tip–sample distance (1–20) nm, sample thickness (0–5) μm and dielectric constant (1–20), using the numerical simulation of the equivalent charge method. For potential heterogeneities on metallic surfaces expressions are in agreement with the bibliography. The lateral resolution of samples having a dielectric constant of more than 10 tends to metallic behaviour. We found a characteristic thickness of 100 nm, above which the lateral resolution measured on the dielectric surface is close to that of an infinite medium. As previously reported, the lateral resolution is better in the gradient mode than in the force mode. Finally, we showed that for the same experimental conditions, the lateral resolution is better for a polarizable particle than for a charge, i.e. dielectric heterogeneities should always look 'sharper' (better resolved) than inhomogeneous charge distributions. This fact should be taken into account when interpreting images of heterogeneous samples.

(Some figures in this article are in colour only in the electronic version)

1. Introduction

Electrostatic force microscopy (EFM) permits one to study the electrical properties of surfaces at the nanoscale by applying a voltage between the tip of the microscope and the sample. EFM has been largely used to study surface potential and capacitance [1–6], charge or dopant distribution [7–11] and polarization forces on dielectric surfaces [12, 13]. It permits probing of the conducting properties of carbon nanotubes [14–16], study of liquid surfaces [17] or induction of capillary condensation of water bridges between the tip and sample [18]. EFM has thus become an important tool to characterize the electrical and electrochemical properties of metals, semiconductors, dielectrics and organic materials at the nanoscale.

As in other scanning probe microscopy (SPM) techniques, the interpretation of the EFM images is not always evident [19]. The force mode (amplitude modulation, AM)

 © 2011 IOP Publishing Ltd Printed in the UK & the USA

is sensitive to long range electrostatic forces and involves the contribution of the cone and cantilever (stray contribution) in addition to the apex area [20]. This phenomenon can lead to errors in the interpretation of images or even contrast inversion in the measured potential [16, 21]. The effective surface potential can be restored if the exact geometry of the probe is known [22, 23]. A recent study has shown that such errors can be lowered by working in the gradient mode (frequency modulation, FM) for which the stray contribution effects and lift height dependence are reduced [24]. Concerning the lateral resolution for metallic surfaces, Belaidi *et al* [25] and Shen *et al* [26] used the same definition: while recording the signal (force or gradient) over a potential discontinuity a step is observed between the two domains; these authors defined the lateral resolution as the difference between the position x_1 where the contribution to the signal is 75% of maximum and the position x_2 where it is close to 25% of the maximum. These authors used finite element simulation and boundary element conditions, respectively, to simulate the electrostatic signal. On the other hand, Gómez-Moñivas *et al* [27] used the generalized image charge method to calculate the response function of the microscope (derivative of the modulus of the square of the normal electric field at the surface towards the tip–sample distance) and defined the lateral resolution as the half width at half maximum of this function. Even if these authors used different types of simulation and definitions, they reached the same qualitative results: for a tip having a given radius R, the lateral resolution Δx for both force and gradient mode is proportional to $(Rd_0)^{1/2}$ (where d_0 is the tip–sample distance) for small distances and varies linearly with d_0 when $d_0 \geqslant R$. Due to the short range characteristic of the force gradient signal, the resolution in gradient mode (involving mainly the apex region) is always better (Δx smaller) than the one in force mode. Furthermore, in agreement with [28], Shen *et al* [26] have shown that this square root dependence is also valid as a function of the tip radius in the gradient mode but that an optimal tip radius exists in the force mode. This phenomenon is attributed to the less sensitive contribution of the conical portion (non-negligible in the force mode) for small tip radius.

In contrast with the relatively well-known metallic samples, the resolution on dielectric samples has not been analysed in detail. Early work [27], based on numerical results, suggested that the EFM lateral resolution was almost independent of the sample dielectric constant, ε_r, at least for the relatively large ε_r values ($\varepsilon_r > 10$). In the last few years, there has been a renewed interest in the experimental study of insulators at the nanoscale and different groups have presented several methods to probe dielectric properties using EFM. First implemented to measure properties in one point [29–31], these methods were soon extended to image dielectric properties [32–34] reaching an experimental value of the lateral resolution $\Delta x \sim 40$ nm. However, the lack of theoretical background does not permit us to interpret this value in terms of dielectric properties ε_r or thickness of the sample h. Our main goal here is to quantify the EFM lateral resolution on dielectric samples as a function of the tip–sample distance d_0 and both sample thickness, h, and dielectric constant, ε_r. We present a numerical study in the force and gradient modes. In agreement with previous results [27], we found that for $\varepsilon_r > 10$ the resolution approaches the metallic sample values, being independent of the dielectric constant. However, as ε_r decreases, there is a significant increase of Δx which is a function of both the geometry and dielectric properties of the sample. Interestingly, even for large dielectric constants, the lateral resolution for inhomogeneous surface potential or surface charge distributions [25, 26] differs from that obtained for inhomogeneous dielectrics. As we will show, while the former (proportional to the applied tip bias voltage) can be obtained from an EFM response function corresponding to a test point charge, the latter (proportional to the squared bias) is given by the response to a test polarizable particle. As a consequence, our results predict that dielectric heterogeneities should always look 'sharper' (better resolved) than inhomogeneous charge distributions.

The paper is structured as follows: we will first introduce the numerical simulation of the equivalent charge method before defining the lateral resolution from the force and gradient on a test charge and a test polarizable particle. We will then study the behaviour of the lateral resolution as a function of the different parameters: tip–sample distance, dielectric thickness and constant.

2. Numerical simulation and definition of the lateral resolution

The principle of numerical simulation in the equivalent charge method (ECM) is presented in [29, 35]. The ECM, in analogy with other 'image charge' methods [36, 37], uses a discrete distribution of image charges that permits us to calculate the potential created by a difference in voltage between a tip and a grounded dielectric. Figure 1(a) represents the potential simulated by a probe having a radius of $R = 30$ nm and half cone angle $\theta = 15°$ at a tip–sample distance $d_0 = 20$ nm. The thickness of the dielectric is $h = 200$ nm and its dielectric constant $\varepsilon_r = 4$. The dielectric permittivity of the air is assumed to be $\varepsilon_0 = 8.854 \times 10^{-12}$ F m^{-1}. The ECM permits us to compute the potential in the three dimensions of the space. We select the potential in the vertical axis of symmetry of the tip ($y = 0$).

The electric field derives from the potential ($\vec{E} = -\text{grad}V$), therefore we are able to compute the electric field from figure 1(a). Figure 1(b) exemplifies the calculation of the normal component of the electric field at the surface, E_z, from the difference between the potential recorded one z-step above the surface and at the surface. This geometric construction shows that, due to the shape of the potential and the definition of the electric field as a gradient, the half width at half maximum of the electric field is smaller than the potential one. Using a similar approach, we are also able to compute the modulus of the electric field: $|\vec{E}| = \sqrt{E_x^2 + E_z^2}$.

Let us consider the tip–sample system sketched in figure 1 as a reference system. Changes in the electrostatic force due to the presence of additional dielectric inhomogeneities on the reference sample can be described as the convolution of the EFM response function and the so-called surface equivalent

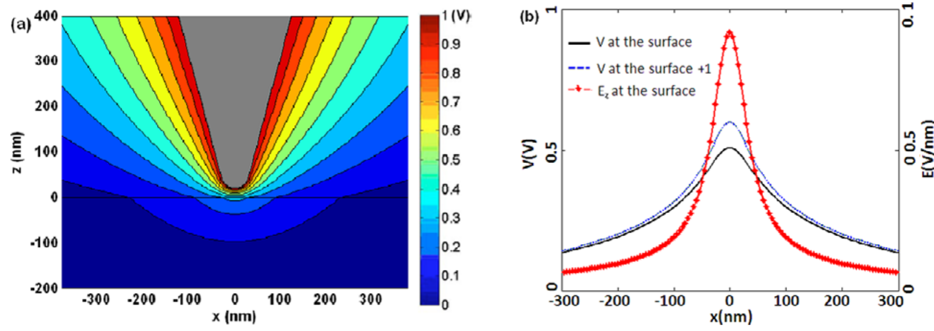

Figure 1. (a) Potential created by a tip ($R = 30$ nm, $\theta = 15°$, $d_0 = 20$ nm) in front of a dielectric ($h = 200$ nm, $\varepsilon_r = 4$) simulated by the ECM. (b) Potential recorded over the surface of the sample (full line), one z-step above (dashed line) and normal electric field (*) at the surface of the sample (difference between the two potentials).

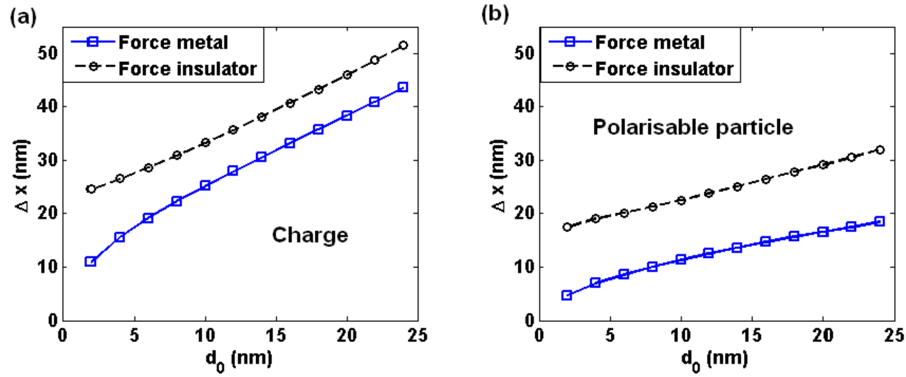

Figure 2. $\Delta x(d_0)$ calculated by the ECM for a metallic surface and an ideal insulator in the force mode for a charge (a) and a polarizable particle (b).

profile [19]. The lateral resolution can be defined as the half width of the 'response function' at the dielectric surface [27]. Physically, the response function corresponds to the additional force due to a 'test' polarizable punctual particle:

$$F_\alpha \propto \frac{\partial}{\partial z}(E_x^2 + E_z^2). \tag{1}$$

Analogously, for a non-uniform free charge distribution on the reference sample, the response function will be proportional to the force on a 'test' point charge, i.e. proportional to the reference electric field,

$$F_q \propto E_Z. \tag{2}$$

It is worth noting that the EFM response function and, as a consequence, the EFM lateral resolution when measuring dielectric inhomogeneities (polarization forces) can be very different from that observed for charge or surface potential inhomogeneities.

Similar arguments can be applied to force gradient measurements, with a response function proportional to the derivative of the force towards the tip–sample distance:

$$G_\alpha \propto \frac{\partial}{\partial d_0}\frac{\partial}{\partial z}(E_x^2 + E_z^2), \tag{3}$$

$$G_q \propto \frac{\partial}{\partial d_0} E_Z. \tag{4}$$

From a numerical point of view, the derivative with respect to d_0 is realized by subtracting the quantities obtained for two different tip–sample distances. The shape of $F_q(x)$, $F_\alpha(x)$, $G_q(x)$ and $G_\alpha(x)$, computed at the sample surface, is qualitatively similar to the one observed for $E_z(x)$ in figure 1(b). From the discussion above, we then define the lateral resolution in the force, Δx_F, and gradient, Δx_G, modes as the half width at half maximum of $F(x)$ and $G(x)$ recorded at the sample surface, respectively.

3. Results and discussion

We are now going to present the results of the study of the lateral resolution in the force and gradient modes for a charge and a polarizable particle as a function of the tip–sample distance d_0, thickness h and dielectric constant ε_r of the sample. We will first study the behaviour as a function of the tip–sample distance for the two limiting cases of a metallic surface and an ideal insulator having a dielectric constant of 1 and an 'infinite' thickness of 5 μm. Then we will focus on the influence of the thickness and dielectric constant for a given value of the tip–sample distance.

3.1. Lateral resolution as a function of the tip–sample distance

Figure 2 represents the lateral resolution calculated by the ECM in the force mode for a metallic surface and an ideal insulator.

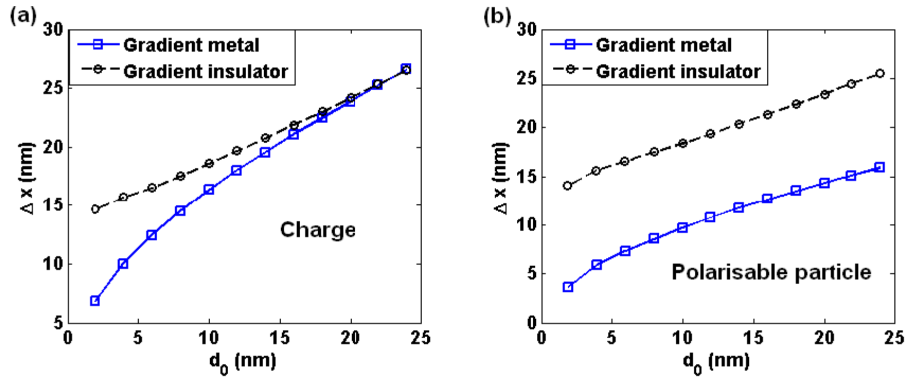

Figure 3. $\Delta x(d_0)$ calculated by ECM for a metallic surface and an ideal insulator in the gradient mode for a charge (a) and a polarizable particle (b).

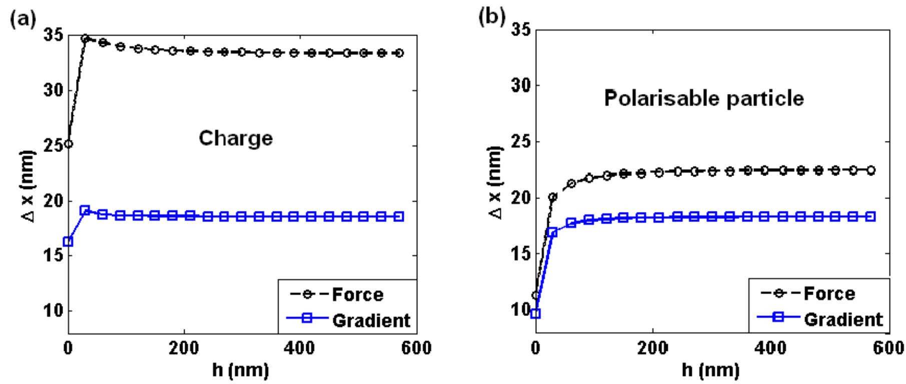

Figure 4. $\Delta x(h)$ calculated by the ECM for an insulator ($\varepsilon_r = 1$) in the force and gradient mode for a charge (a) and a polarizable particle (b) at $d_0 = 10$ nm.

As the behaviour will later be studied at $d_0 = 10$ nm it is interesting to note the value of the resolution at this reference tip–sample distance: in the force mode, the lateral resolution for a test charge simulated by the ECM gives $\Delta x^{\mathrm{m}}_{Fq} = 25.3$ nm for a metallic surface and $\Delta x^{\mathrm{i}}_{Fq} = 33.2$ nm for an ideal insulator; for a polarizable particle we found $\Delta x^{\mathrm{m}}_{F\alpha} = 11.4$ nm and $\Delta x^{\mathrm{i}}_{F\alpha} = 22.5$ nm (figure 2).

Figure 3 represents the lateral resolution in the gradient mode.

In the same experimental conditions, the resolution is always better in the gradient mode than in the force mode. This can be observed by comparing our results at the reference tip–sample distance $d_0 = 10$ nm in the force mode (figure 2, see above) with those obtained in the gradient mode (figure 3): the lateral resolution for a test charge is now $\Delta x^{\mathrm{m}}_{Gq} = 16.3$ for a metallic surface and $\Delta x^{\mathrm{i}}_{Gq} = 18.6$ nm for an ideal insulator; for a polarizable particle we found $\Delta x^{\mathrm{m}}_{G\alpha} = 9.7$ nm and $\Delta x^{\mathrm{i}}_{G\alpha} = 18.4$ nm. As mentioned in section 1, the gradient mode has a shorter range of interaction. This can be understood knowing that the shapes of the profile of the forces recorded at two d_0 steps have a similar qualitative shape to the potential ones recorded at two z steps in figure 1(b). Using the same geometric argument as the one explained for figure 1(b), it appears that the force gradient has a smaller half width at half maximum than the force. One consequence of this phenomenon is that the interaction is mainly concentrated on the apex in the gradient mode whereas the cone has a more important influence in the force mode, as has been shown for metallic surfaces in [38, 39]. This fact is also confirmed by the results presented in figure 5(b) of [26] where the authors show that the lateral resolution increases with the cone angle in the force mode whereas almost no dependence is observed in the gradient mode. The force on a polarizable particle is also defined with a derivative towards z and dominated by the normal component of the electric field to the square ($E_x < E_z$ in equation (2)). Both square and derivative will lead to a sharper profile (i.e. a better lateral resolution) for a polarizable particle than for the charge.

In figures 2 and 3 it appears that for a charge on a metallic surface, in agreement with the literature [2–5], the lateral resolution is proportional to $(Rd_0)^{1/2}$ for $d_0 < R/3$ and then varies linearly with the tip–sample distance for both force and gradient modes. The same behaviour is observed for a polarizable particle. However, we note that the lateral resolution of an ideal insulator has a linear dependence over the whole range of tip–sample distance leading to a non-null value of the lateral resolution in contact ($d_0 = 0$ nm).

3.2. Lateral resolution as a function of the sample parameters (h, ε_r)

Figure 4 represents the lateral resolution in both force and gradient modes as a function of the thickness for an insulator

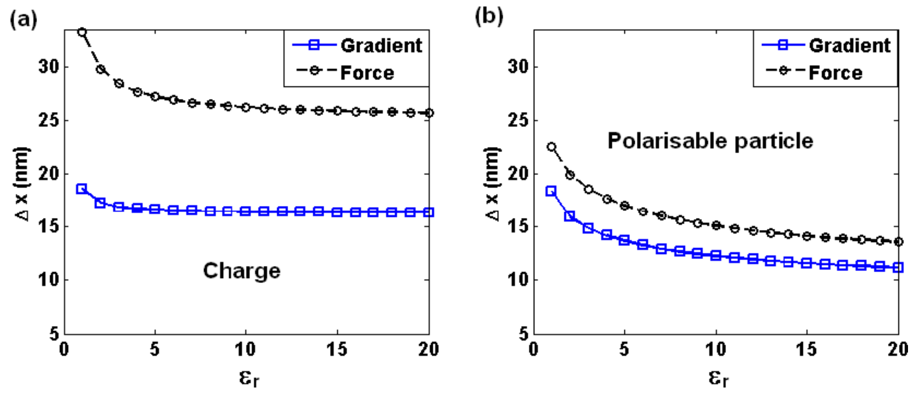

Figure 5. $\Delta x(\varepsilon_r)$ calculated by the ECM for an insulator ($h = 5\ \mu$m) in the force and gradient mode for a charge (a) and a polarizable particle (b) at $d_0 = 10$ nm.

($\varepsilon_r = 1$) recorded at a tip–sample distance of 10 nm. The lateral resolution simulated by the ECM quickly increases from the value of a metallic surface at $h = 0$ nm ($\Delta x^{\rm m}_{Fq} = 25.3$ nm and $\Delta x^{\rm m}_{Gq} = 16.3$ nm for a charge, see figure 4(a), and $\Delta x^{\rm m}_{F\alpha} = 11.4$ nm and $\Delta x^{\rm m}_{G\alpha} = 9.7$ nm for a polarizable particle, figure 4(b)) to the one of an 'infinite' dielectric ($\Delta x^{\rm i}_{Fq} = 33.2$ nm and $\Delta x^{\rm i}_{Gq} = 18.6$ nm for a charge, see figure 4(a), and $\Delta x^{\rm i}_{F\alpha} = 22.5$ nm and $\Delta x^{\rm i}_{G\alpha} = 18.4$ nm for a polarizable particle, figure 5(b)). Therefore, we can define a limit thickness of about 100 nm above which the value of the lateral resolution is close that of an infinite medium.

Figure 5 represents the lateral resolution in the force and gradient modes as a function of the dielectric constant for both a charge and a polarizable particle. The dielectric medium has been simulated with a thickness of 5 μm. The lateral resolution is decreasing from the value of an ideal insulator ($\Delta x^{\rm i}_{Fq} = 33.2$ nm and $\Delta x^{\rm i}_{Gq} = 18.6$ nm for a charge, figure 5(a), and $\Delta x^{\rm i}_{F\alpha} = 22.5$ nm and $\Delta x^{\rm i}_{G\alpha} = 18.4$ nm for a polarizable particle, figure 5(b)) and tends to the value of a metallic surface ($\Delta x^{\rm m}_{Fq} = 25.3$ nm and $\Delta x^{\rm m}_{Gq} = 16.3$ nm for a charge, figure 5(a), and $\Delta x^{\rm m}_{F\alpha} = 11.4$ nm and $\Delta x^{\rm m}_{G\alpha} = 9.7$ nm for a polarizable particle, figure 5(b)). For $\varepsilon_r = 10$, the values of the lateral resolution simulated by the ECM for a charge in the force and gradient mode approach the metallic limit at 4% and 1%, respectively. For a polarizable particle, the lateral resolution tends more slowly to the limit value: for the same value of $\varepsilon_r = 10$ the discrepancy with the metallic limit is still 24% for the force and 20% for the gradient.

4. Conclusion

We have introduced a definition of the lateral resolution Δx in electrostatic force microscopy from the force response to a 'test' point charge or a 'test' polarizable particle at the surface of dielectric samples. We have shown that the lateral resolution measured on inhomogeneous dielectrics should be better than that obtained when measuring inhomogeneous surface charges and potentials. We used the numerical simulation of the equivalent charge method to study the behaviour of Δx in the force and gradient modes as a function of the tip–sample distance d_0, thickness h and dielectric constant ε_r of the sample. Due to its short range interaction, the lateral resolution is better in the gradient mode than in the force mode. In agreement with the literature [25–27], we showed that for a metallic surface, $\Delta x(d_0)$ has a square root dependence for small tip–sample distances ($\Delta x(d_0) < R/3$) and then behaves linearly. However, for an insulator, the lateral resolution exhibits a linear dependence over the whole range of tip–sample distances leading to a non-null value in contact. For a given value of the dielectric constant, $\Delta x(h)$ quickly increases from the limit value of the metallic surface ($h = 0$) to that of an 'infinite' sample ($h = 5\ \mu$m). We can therefore define a thickness of 100 nm above which the lateral resolution can be considered as that of an infinite medium in typical experimental conditions. For a given value of the thickness, $\Delta x(\varepsilon_r)$ decreases from the limit value of an ideal insulator ($\varepsilon_r = 1$) to that of a metallic surface (ε_r tends to infinity). For a charge, the lateral resolution of sample having a dielectric constant of 10 has a value very close to the infinite limit (less than 4% difference) whereas we observe a slower variation for the polarizable particle: a discrepancy of about 25% is still observed for $\varepsilon_r = 10$. Finally we showed that for the same experimental conditions the lateral resolution is better for a polarizable particle than for a charge. This fact should be taken into account in the interpretation of heterogeneous samples in EFM images.

Acknowledgments

CR and JJS acknowledge interesting discussions with G Lévêque and G Gomila, G M Sacha, E Sahagún, respectively. This work was supported by the Donostia International Physics Center (DIPC), the Basque Country Government (ref. no. IT-436-07, Depto. Educación, Universidades e Investigación), the Comunidad de Madrid Microseres-CM Project (S2009/TIC-1476), the Spanish Ministry of Science and Innovation (grant no. MAT 2007-63681 and FIS2009-13430-C01-C02) and the European Soft Matter Infrastructure (ESMI) Programme.

References

[1] Bugg C D and King P J 1998 *J. Phys. E: Sci. Instrum.* **21** 147
[2] Williams C C, Hough W P and Rishton A 1989 *Appl. Phys. Lett.* **55** 203

[3] Lányi S, Torok J and Rehurek P 1996 *J. Vac. Sci. Technol.* B **14** 892
[4] Martin Y, Abraham D W and Wickramasinghe H K 1998 *Appl. Phys. Lett.* **52** 1103
[5] Nonnenmacher M, O'Boyle M and Wickramasinghe H K 1992 *Ultramicroscopy* **42–44** 268
[6] Hochwitz T, Henning H K, Leveg C, Daghlian C and Slinkman J 1996 *J. Vac. Sci. Technol.* B **14** 457
[7] Williams C C, Slinkman J, Hough W P and Wickramasinghe H K 1989 *Appl. Phys. Lett.* **55** 1662
[8] Barrett R C and Quate C F 1992 *Ultramicroscopy* **42–44** 262
[9] Stern J E, Terris B D, Mamin H J and Rugar D 1998 *Appl. Phys. Lett.* **53** 2717
[10] Terris B D, Stern J E, Rugar D and Mamin H J 1989 *Phys. Rev. Lett.* **63** 2669
[11] Schonenberger C and Alvarado S 1990 *Phys. Rev. Lett.* **65** 3162
[12] Hao H W, Baró A M and Sáenz J J 1991 *J. Vac. Sci. Technol.* B **9** 1323
[13] Hu J, Xiao X D and Salmeron M 1995 *Appl. Phys. Lett.* **67** 476
[14] Bachtold A, Fuhrer M S, Plyasunov S, Forero M, Anderson E H , Zettl A and McEuen P L 2000 *Phys. Rev. Lett.* **84** 6082
[15] Sacha G M, Gómez-Navarro C, Sáenz J J and Gómez-Herrero J 2006 *Appl. Phys. Lett.* **89** 173122
[16] Zaho M, Gu X, Lowther S E, Park C, Jean Y C and Nguyen T 2010 *Nanotechnology* **21** 225702
[17] Verdaguer A, Sacha G M, Bluhm H and Salmeron M 2006 *Chem. Rev.* **106** 1478
[18] Gómez-Moñivas S, Sáenz J J, Calleja M and García R 2003 *Phys. Rev. Lett.* **91** 056101
[19] Gómez-Moñivas S, Sáenz J J, Carminati R and Greffet J J 2000 *Appl. Phys. Lett.* **76** 2955–7
[20] Glatzel T, Sadewasser S and Lux-Steiner M Ch 2003 *Appl. Surf. Sci.* **210** 84–9
[21] Henning A K, Hochwitz T, Slinkman J, Never J, Hoffmann S, Kaszuba P and Daghlian P 1995 *J. Appl. Phys.* **77** 1888–96
[22] Strassburg E, Boag A and Rosenwaks Y 2005 *Rev. Sci. Instrum.* **76** 083705
[23] Charrier D S H, Kemerink M, Smalbrugge B E, de Vries T and Janssen R A J 2008 *ACS Nano* **2** 622–6
[24] Ziegler D and Stemmer A 2011 *Nanotechnology* **22** 075501
[25] Belaidi S, Lebon F, Girard P, Lévêque G and Pagano S 1998 *Appl. Phys.* A **66** S239–43
[26] Shen Y, Lee M, Lee W, Barnett D M, Pinsky P M and Prinz F B 2008 *Nanotechnology* **19** 035710
[27] Gómez-Moñivas S, Froufe L S, Carminati R, Greffet J J and Sáenz J J 2001 *Nanotechnology* **12** 496–9
[28] Jacobs H O, Leuchtmann P, Homan O J and Stemmer A 1998 *J. Appl. Phys.* **84** 1168–73
[29] Riedel C, Arinero R, Tordjeman Ph, Ramonda M, Lévêque G, Schwartz G A, de Oteya D G, Alegría A and Colmenero J 2009 *J. Appl. Phys.* **106** 024315
[30] Crider P S, Majewski M R, Zhang J, Oukris H and Israeloff N E 2007 *Appl. Phys. Lett.* **91** 013102
[31] Fumagalli L, Gramse G, Esteban-Ferrer D, Edwards M A and Gomila G 2010 *Appl. Phys. Lett.* **96** 183107
[32] Gramse G, Casuso I, Toset J, Fumagalli L and Gomila G 2009 *Nanotechnology* **20** 395702
[33] Riedel C, Sweeney R, Israeloff N E, Arinero R, Schwartz G A, Alegria A, Tordjeman Ph and Colmenero J 2010 *Appl. Phys. Lett.* **96** 213110
[34] Riedel C, Arinero R, Tordjeman Ph, Lévêque G, Schwartz G A, Alegría A and Colmenero J 2010 *Phys. Rev.* E (R) **81** 010801
[35] Riedel C, Arinero R, Tordjeman Ph, Lévêque G, Schwartz G A, de Oteya D G, Alegría A and Colmenero J 2010 *Eur. Phys. J. Appl. Phys.* **50** 10501
[36] Mesa G, Dobado-Fuentes E and Sáenz J J 1996 *J. Appl. Phys.* **79** 3944
[37] Sacha G M, Sahagún E and Sáenz J J 2007 *J. Appl. Phys.* **101** 024310
[38] Colchero J, Gil A and Baró A M 2001 *Phys. Rev.* B **64** 245403
[39] Gil A, Colchero J, Gómez-Herrero J and Baró A M 2003 *Nanotechnology* **14** 332